

Study of Superheavy Elements at the GSI-SHIP

S. Hofmann,^{*,a} D. Ackermann,^a S. Antalic,^b H.G. Burkhard,^a R. Dressler,^c F.P. Heßberger,^a B. Kindler,^a I. Kojouharov,^a P. Kuusiniemi,^d M. Leino,^d B. Lommel,^a R. Mann,^a G. Münzenberg,^a K. Nishio,^e A.G. Popeko,^f S. Saro,^b H.J. Schött,^a B. Streicher,^b B. Sulignano,^a J. Uusitalo,^d and A.V. Yeremin^f

^aGesellschaft für Schwerionenforschung (GSI), D-64220 Darmstadt, Germany

^bDepartment of Nuclear Physics, Comenius University, SK-84248 Bratislava, Slovakia

^cPaul Scherrer Institut, 5232 Villigen, Switzerland

^dDepartment of Physics, University of Jyväskylä, FIN-40351 Jyväskylä, Finland

^eJAEA, Tokai, Ibaraki 319-1195, Japan

^fFlerov Laboratory of Nuclear Reactions, JINR, Ru-141 980 Dubna, Russia

Received: December 26, 2005

An overview of present experimental investigation of superheavy elements is given. The data are compared with theoretical descriptions. Results are reported from an experiment to confirm production of element 112 isotopes in irradiation of $^{238}\text{UF}_4$ with ^{48}Ca . One spontaneous fission event was measured, which agrees with three events of previously measured data which had been assigned to the decay of $^{283}112$. However, more experimental work is needed in order to obtain an independent and unambiguous confirmation of previous results.

1. Introduction and status of experiments

For the synthesis of heavy and superheavy elements (SHE) fusion-evaporation reactions are used. Two approaches have been successfully employed. Firstly, reactions with medium mass ion beam impinging on targets of stable Pb and Bi isotopes (cold fusion). These reactions have been successfully used to produce elements up to $Z=112$ at GSI¹ and to confirm these experiments at RIKEN² and LBNL.³ Using a ^{209}Bi target the isotope $^{278}113$ was recently synthesized at RIKEN.² Secondly, reactions between lighter ions, especially with beams of ^{48}Ca , and radioactive actinide targets (hot fusion) have been used to produce more neutron rich isotopes of elements from $Z=112$ to 116 and 118 at FLNR.⁴ Figure 1 summarizes the data as they are presently known or under investigation.

Besides the discovery of the existence of these high- Z elements, two more important observations emerged. Firstly, the expectation that half-lives of the new isotopes should lengthen with increasing neutron number as one approaches the island of stability seems to be fulfilled. Secondly, the measured cross-sections for the relevant nuclear fusion processes reach values up to 5 pb, which is surprisingly high. Furthermore, they seem to be correlated with the variation of shell-correction energies as predicted by macroscopic-microscopic calculations.^{5,6}

A number of excitation functions were measured for the synthesis of elements from nobelium to darmstadtium using cold fusion reactions. Some of the curves are shown together with the two data points for $^{277}112$ in Figure 2. Maximum evaporation residue cross-sections (1n channel) were measured at beam energies well below a contact configuration, where projectile and target nucleus come to rest according to the fusion model by Bass.⁷

Excitation functions for hot fusion reactions were measured recently at FLNR.⁴ The data for the reaction $^{48}\text{Ca} + ^{244}\text{Pu} \rightarrow ^{288}114 + 4n$ is shown in the lowest panel in Figure 2. Here the peak is located well above the contact configuration calculated

from a mean value of the nuclear potential of the deformed target nucleus. This shift as well as the increased width of the curve (10.6 MeV instead of 4.6 MeV FWHM for ^{265}Hs) are in accord with an orientation effect on fusion using a deformed target nucleus. The shift to higher energy indicates collisions in direction of the short deformation axis.

It was pointed out in the literature⁹ that closed shell projectile and target nuclei are favorable for the synthesis of SHEs.

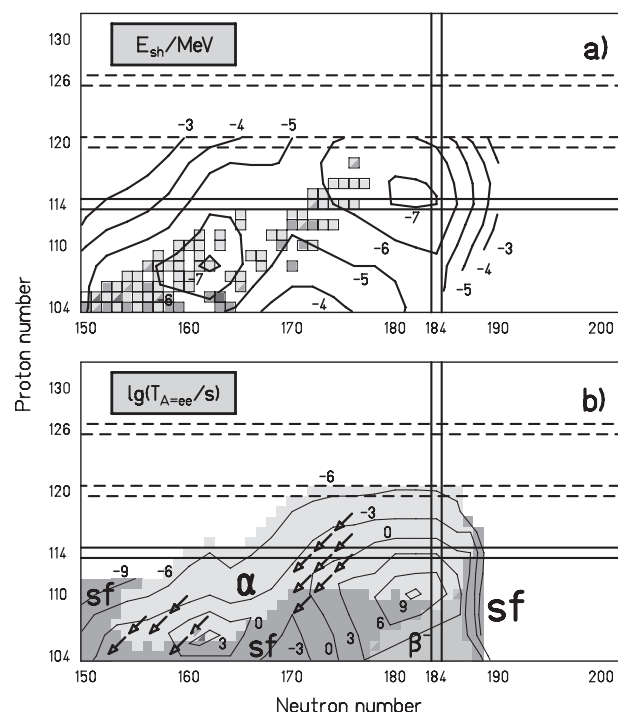


Figure 1. Calculated ground-state shell correction energy (a) and dominating partial half-lives for α , β^+ or EC, β^- decay, and spontaneous fission (SF) of even-even nuclei (b). The calculated data were taken from References 5 and 6. The squares in (a) show the isotopes of heavy and superheavy elements, which are known or presently under investigation, and the arrows in (b) mark the measured decay chains. In all cases the decay chains end, in agreement with theoretical predictions, at nuclei decaying by SF.

*Corresponding author. E-mail: S.Hofmann@gsi.de. "Josef Buchmann Professor Laureatus"

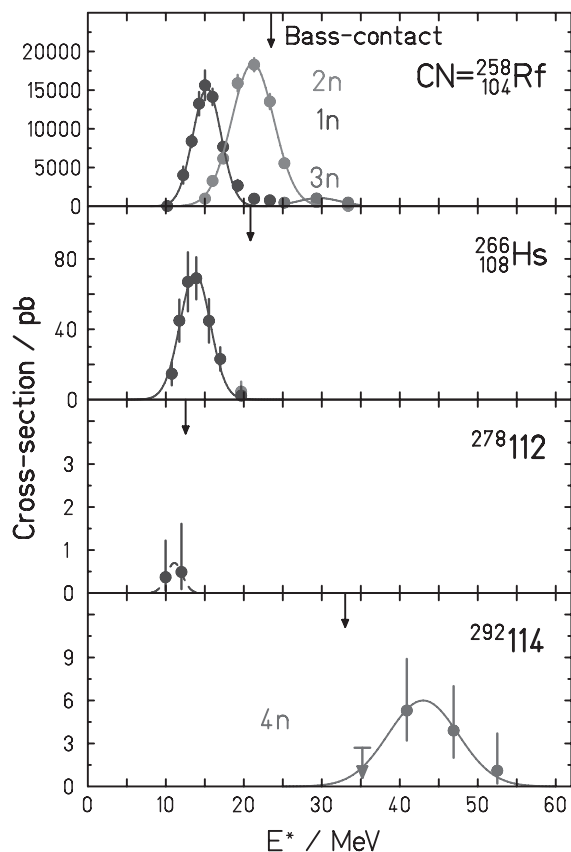


Figure 2. Excitation functions measured at SHIP for the synthesis of elements Rf and Hs plus two data points measured for $Z=112$ using cold fusion reactions¹ (^{208}Pb target) and at the DGFERS of FLNR for the synthesis of element $Z=114$ using hot fusion reaction (^{244}Pu target). The arrows mark the excitation energy for reactions, when the kinetic energy of the projectile is just sufficient high to reach a contact configuration according to the fusion model by Bass.⁷ The excitation energies were calculated using binding energies for the compound nuclei from Reference 8.

The reason is not only a low (negative) reaction Q -value and thus a low excitation energy, but also that fusion of such systems is connected with a minimum of energy dissipation. The fusion path proceeds along cold fusion valleys, where the reaction partners maintain kinetic energy up to the closest possible distance. Recent theoretical studies are able to reproduce the measured data. That work is continued by various groups (see e.g. References 10,11, and references therein) aiming to work out reliable predictions for the production cross-sections of SHEs.

2. Study of the $^{48}\text{Ca} + ^{238}\text{U}$ Reaction

2.1. Results from previous investigations. Data from studies of the reaction $^{48}\text{Ca} + ^{238}\text{U} \rightarrow ^{286}112^*$ are contradictory concerning half-lives and cross-sections. A summary of the published data is shown in Table 1.

Most comprehensive studies of hot fusion reactions with ^{48}Ca beams were performed at the DGFERS of FLNR, see Reference 4. The results from this group are based not only on the reaction $^{48}\text{Ca} + ^{238}\text{U}$, but also on data from reactions for the synthesis of nuclei of elements beyond $Z=112$. These data served as a basis for the preparation of our experiment to search for $^{283}112$ at SHIP using the reaction $^{48}\text{Ca} + ^{238}\text{U}$.

2.2. Technical aspects and test reactions. The ^{48}Ca beam was prepared from the ECR ion source and accelerator UNILAC at GSI. Metallic, isotopically enriched (89.5%) ^{48}Ca and the ECR oven technique were used. Ions with charge state 10+ were extracted and accelerated by the high charge state injector (RFQ + IH structure) and the UNILAC to Coulomb barrier energies. A mean current of 1.2 μA was reached on target at a duty factor of 28% (5.5 ms wide pulses at 20 Hz repetition frequency). The consumption of ^{48}Ca was 0.6 mg/h on the average.

The targets were prepared from the chemical compound UF_4 . Layers of 488, 408, and 451 $\mu\text{g}/\text{cm}^2$ were evaporated on backing foils of 42 $\mu\text{g}/\text{cm}^2$ C and subsequently covered with C layers of 10 or 20 $\mu\text{g}/\text{cm}^2$. Details of the target preparation are given in Reference 16. The target thickness was controlled on-line by registration of elastically scattered projectiles and scattering of 20 keV electrons.¹⁷ The data showed a continuous decrease of the thickness during irradiation. The target wheel was replaced at the latest, when the losses reached a value of 30%. We estimated a mean fading of 20% of target thickness for the calculation of the cross-section. A total of 14 uranium target wheels were used. The uranium content of new and irradiated targets including the performance of the whole experimental set-up was tested by measuring the yield of fusion products from reactions with a ^{22}Ne beam supplied for two days at half time of the experiment. This test confirmed the results obtained by the measurements using scattered projectiles or electrons.

Properties of SHIP and of the detector system are described in Reference 1. Since that time, however, the detector system was modified. A Si veto detector was mounted behind the stop detector and the Ge detectors were replaced by a four crystal Ge clover detector. The new set-up is shown in Figure 3. During the uranium irradiation the first of the TOF detectors was removed after few days, which resulted in reduced scattering of the ions and deeper implantation into the Si stop detector.

Table 1: Published data from investigation of the reaction $^{48}\text{Ca} + ^{238}\text{U} \rightarrow ^{286}112^*$.

Duration / day	E^* / MeV	dose / 10^{18}	events	event type	$T_{1/2}$ / s	xn	σ / pb	Ref.
25	33	3.5	2	ER-SF	81	3	5.0	12
15	39	2.2	0	—	—	—	< 7.3	12
29	33	5.9	0	—	—	—	< 2.2	13
15	35.5	4.7	2	ER-SF	568	3	3.0	13
14	31.4	5.8	1	ER-(α)-SF	(3.4)	3	0.5	4
17	35.0	7.1	2	ER-(α)-SF	(1.4)	3	2.5	4
			3	ER- α -SF	2.7	3		
			1	ER-4 α -SF	6.1	3		
13	39.8	5.2	1	ER-SF	0.00014	4	0.6	4
22.5	34.2	2.8	7	SF	≥ 60	3	2	14
≈ 8.7	31.9	2.26	0	—	—	—	< 0.80	15
≈ 7.1	36.3	1.85	0	—	—	—	< 0.96	15

E^* at half thickness of the target layer; cross-section limits given are “one-event” limits which do not include errors from statistical fluctuations.

Two different field settings for SHIP were calculated using a Monte Carlo method, in order to optimize efficiency for the separation of fusion products from the $^{48}\text{Ca} + ^{238}\text{UF}_4$ reaction. Values of 17% and 24% were obtained. Test reactions using a ^{208}Pb target confirmed the dependence and, because the background did not increase more than proportional, we used the setting with higher efficiency.

The response of the detector system to SF events was investigated especially carefully, expecting that fission will terminate the decay chains of element 112 isotopes. These measurements were performed using the ^{48}Ca beam and targets of ^{208}Pb and ^{206}Pb before and after the main irradiation, respectively. Half time the main irradiation the reaction $^{22}\text{Ne} + ^{238}\text{UF}_4$ was also used for testing purposes. The isotopes produced were ^{254}No , ^{252}No and $^{255,256}\text{No}$, ^{256}Md (p3n channel) and their daughter products, respectively. In order to give an impression of the detector response, we plot in Figure 4 part of the data.

The response of the Ge clover detector to SF was obtained from 10,000 SF events. SF- γ coincidences were measured with fractions of 25.6, 31.0, 23.8, and 7.7% for signals in 1, 2, 3, or all 4 of the 4 Ge crystals, respectively. Only in 11.0% of all cases no signal from the clover detector was in coincidence with SF. Vice versa the response of the clover detector to background events was also measured. From 19,000 background events in the Si stop detector with energies >150 MeV the corresponding fractions are 1.8, 0.4, 6×10^{-4} , 5×10^{-5} , and 97.7%.

2.3. The experiment at SHIP. The irradiations at SHIP, including various test reactions, took place from April 6 to June 9, 2005. Duration of the $^{238}\text{UF}_4$ irradiation, beam energies, beam doses, and results are summarized in Table 2. Chronologically, energies were chosen as given in the table from top to bottom.

No SF events were measured at excitation energies of 37.0 and 32.0 MeV. At the beginning of the irradiation at $E^* = 34.5$ MeV within 12 hours after the test reaction $^{22}\text{Ne} + ^{238}\text{UF}_4$, we measured 3 SF events. The period of interest is shown in Figure 5. The TKE (energy calibration based on α particles) of these SF events is 149.4, 141.3, and 154.8 MeV, respectively, which agrees well with the energies of SF events from ^{255}No or ^{256}Fm measured during the test reaction. We assign these events to the decay of ^{256}Fm on the basis of well known half-lives and SF branching ratios.

A forth SF event was measured on May 8, 2005, also shown in Figure 5. The measured parameters clearly identify this event as SF. The energies, based on α calibration, are $E_{\text{stop}} = 190.4$ MeV and $E_{\text{box}} = 15.3$ MeV. These data are shown together with the energies from SF of ^{252}No in Figure 4. The considerable high TKE is clearly visible. In order to determine the true TKE we used the known TKE of the ^{252}No decay, which is 195 MeV¹⁸ (see Figure 7). The difference to the peak position at 158.7 MeV in Figure 4 is 36 MeV. This energy difference was added to the TKE of the SF event from May 8, which resulted in a TKE of 242 MeV. Assuming a width of the TKE distribution similar to that of ^{252}No , we determine a one σ uncertainty of ± 15 MeV for this one event.

The following properties of the SF event were measured further: no signals from the TOF detectors, signals of 386 and 2068 keV in two of the Ge detectors, appearance during the beam pause at 12.508 ms after beginning of the macro-pulse period which starts with the 5.5 ms wide beam pulse. Finally, the event occurred in strip number 9 of the 16 strip stop detector.

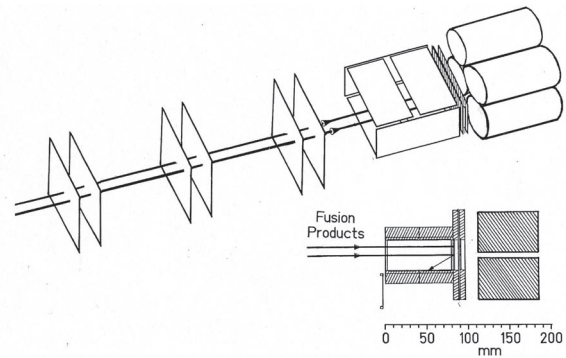


Figure 3. Detector set-up at SHIP. For details see text and description in Reference 1.

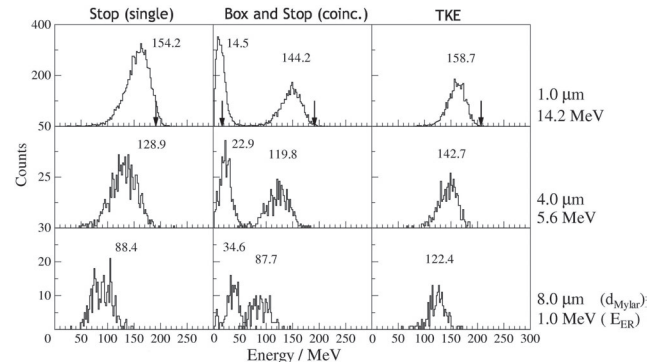


Figure 4. Detector response to SF events of ^{252}No produced in the reaction $^{48}\text{Ca} + ^{206}\text{Pb}$ for three different implantation depth obtained by mylar degrader foils of 1, 4, and 8 μm thickness located in front of the Si detector array. The measured energy (α calibration) of the implanted nuclei is given on the right. The three columns show from the left the energy singles spectra obtained from the stop detector, coincident signals detected in the box and the stop detector (here combined in one spectrum) and the total kinetic energy (TKE) as sum of the coincident signals. The energy values given in MeV are the peaks centre of gravity. The energy calibration is based on α particles and does not include heavy ion deficit energies. Note that at 14.2 MeV implantation energy both fission fragments are detected simultaneously in the stop and the box detector with a probability of 42% relative to all SF signals in the stop detector. This probability is slightly increasing at less deep implantation, because then the probability decreases that both SF fragments are stopped in the stop detector. The arrows in the first row mark the energy values measured from the SF event on May 8, 2005. The implantation energy was 19.5 MeV (see Figure 6), which corresponds roughly to the same implantation depth as for ^{252}No shown in row one, assuming implantation of a heavy isotope of element 112.

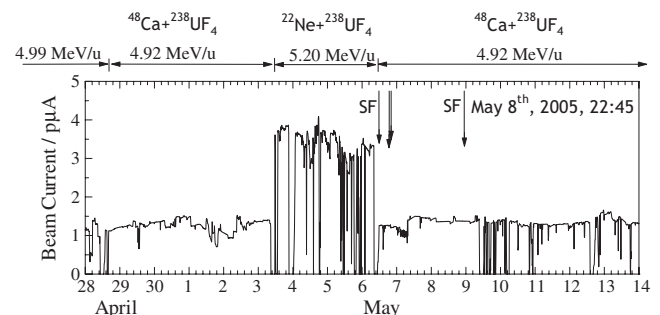


Figure 5. Mean beam currents in particle μA and appearance of SF events during irradiation of an $^{238}\text{UF}_4$ target with ^{48}Ca projectiles. From May 3 to 6 a ^{22}Ne beam was used for testing purposes.

Table 2: Parameters and results of the $^{48}\text{Ca} + ^{238}\text{UF}_4$ irradiation studied at SHIP.

Duration / day	$E_{\text{proj}} / \text{MeV}$	E^* / MeV	dose / 10^{18}	event	event type	$T_{1/2} / \text{s}$	xn	σ / pb
20.9	239.3	37.0	12	0	—	—	—	<0.6
16.8	236.2	34.5	10	1	ER-SF	5.2	?	$0.7^{+1.6}_{-0.6}$
14.8	233.3	32.0	7	0	—	—	—	<0.8

For E^* and cross-section limits see footnote to Table 1.

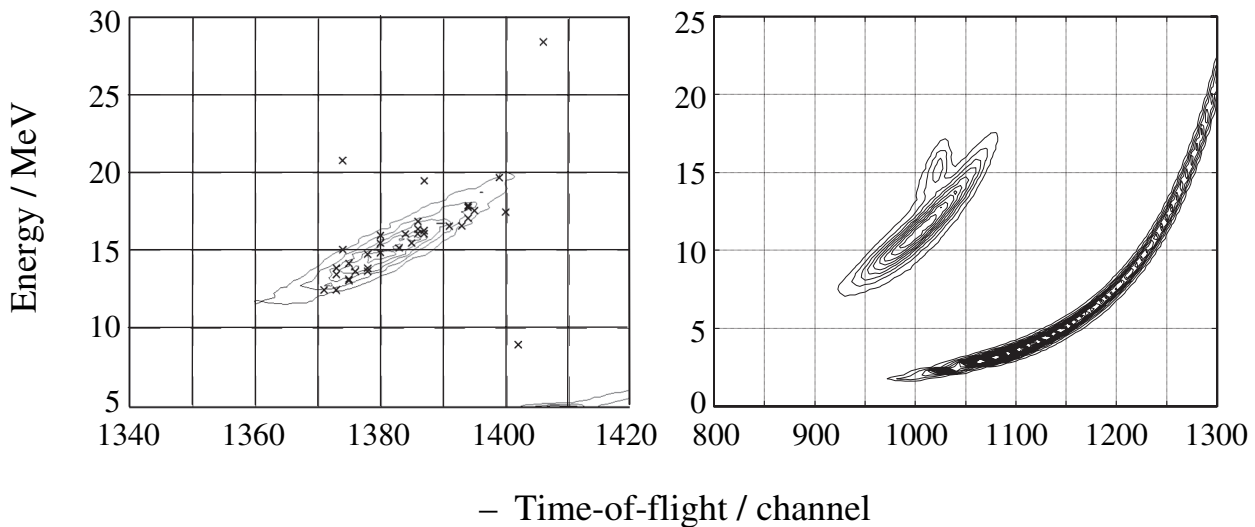


Figure 6. TOF (inverse time scale)–energy spectrum from the reaction $^{48}\text{Ca} + ^{238}\text{UF}_4$ with all signals (marked by crosses) appearing 1000 s before the SF event from May 8, 2005 and within a position window of ± 1 mm (left side) in comparison with a similar plot from the test reaction $^{48}\text{Ca} + ^{206}\text{PbS}$ (right side). In that plot the branches show, with increasing energy, scattered projectiles, scattered target nuclei and ^{252}No evaporation residues. It was taken from an 11.5 hours irradiation in which a beam dose of 3.4×10^{17} was reached. Contour lines begin at 201 counts and are plotted in steps of 201 counts. The structure on the projectile branch is an artifact from the graphics program. The contour lines on the left plot begin with 49 counts and are plotted in steps of 49 counts. For this underlying contour plot all data of the $^{238}\text{UF}_4$ irradiation at 236.2 MeV beam energy were taken, which were measured after the test with the ^{22}Ne beam during a period of 12.1 days and at a beam dose of 7.1×10^{18} projectiles.

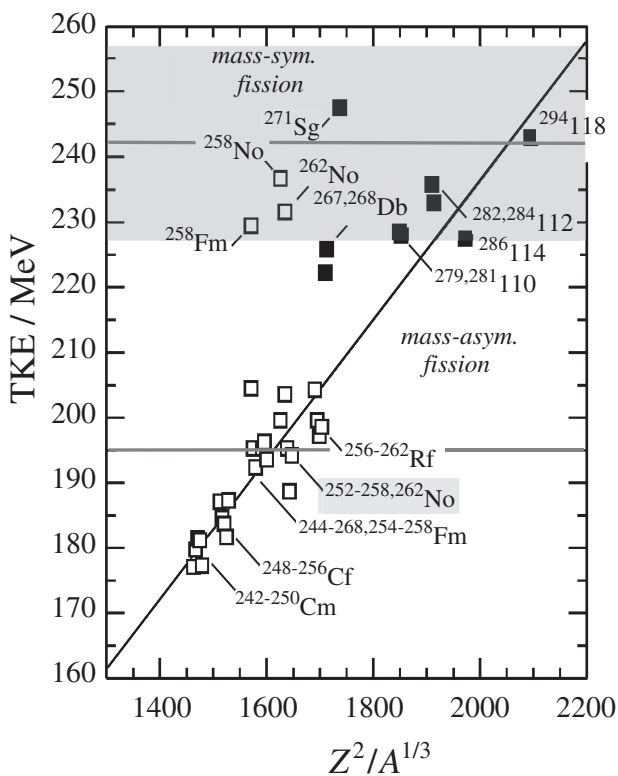


Figure 7. Shown is the Viola-Seaborg systematic of SF nuclei. The horizontal line at 242 MeV marks the TKE value of the SF event measured on May 8 in our experiment. The $\pm 1\sigma$ uncertainty of the mean TKE for this SF decay is also given. Marked at 195 MeV is the TKE of ^{252}No ,¹⁸ which was used for calibration. The TKE of our event was added to a figure taken from Reference 4, which shows data recently measured at FLNR (filled squares) and previously measured data¹⁹ (open squares).

tor at a vertical position of 30 mm from the bottom. The signal from the 28 segment box detector was derived from segment number 13.

At the position of the SF event in the stop detector we searched for preceding α particles and the implanted evaporation residue. Within a reasonable position window of ± 1 mm (a more accurate position calibration is in preparation) and a

time window of 1000 s, we found a total of 36 implantations, but no α particle was measured. Due to the low discriminator level (200 keV) for detection of α particles escaping from the stop detector, we exclude non-registration of such events with high probability. TOF and energy values of the 36 implanted nuclei are plotted in Figure 6, left side. Most of the events coincide with background events from elastically scattered target nuclei. Only one appears at a position where we expect signals from implanted evaporation residues. Where this region is located relative to the background distribution is clearly seen in Figure 6, right side, which was taken from the test reaction $^{48}\text{Ca} + ^{206}\text{PbS}$. The measured time difference between implantation and SF is 7.57 s, which corresponds to a half-life of $(5.2^{+25.1}_{-2.4})$ s.

Finally, we show in Figure 7 the Viola-Seaborg systematic of SF nuclei.

3. Conclusion and Outlook

The data measured for the decay of nuclei in the region of heavy and superheavy nuclei agree well with the predictions from the macroscopic-microscopic model. Using fission barriers from these models, the production cross-sections were reasonably well described in recent theoretical work. Aiming at confirmation of results on element 112 using hot fusion reaction, we measured one SF event which agrees with data measured in Dubna. However, if we tentatively assign the SF to the isotope $^{283}112$ in accordance with the interpretation given in Reference 4, then we have to introduce an adequate SF branching of this nucleus, because no α particle was measured between implantation and SF. More experimental work is needed in order to obtain an independent and unambiguous confirmation of previous results. As a next step we will explore the production of metallic uranium targets which result in higher efficiency of the SHIP separator than targets of chemical compounds, in order to study the reaction $^{50}\text{Ti} + ^{238}\text{U} \rightarrow ^{288}114^*$ and to repeat the reaction $^{48}\text{Ca} + ^{238}\text{U} \rightarrow ^{286}112^*$ under further improved conditions.

Acknowledgement. We thank the UNILAC staff for excellent performance of the ^{48}Ca beam with respect to high stability, high current, and low consumption of material.

References

- (1) S. Hofmann and G. Münzenberg, *Rev. Mod. Phys.* **72**, 733 (2000).
- (2) K. Morita, K. Morimoto, D. Kaji, T. Akiyama, A. Goto, H. Haba, E. Ideguchi, R. Kanungo, K. Katori, H. Koura, H. Kudo, T. Ohnishi, A. Ozawa, T. Suda, K. Sueki, H. Xu, T. Yamaguchi, A. Yoneda, A. Yoshida, and Y.-L. Zhao, *J. Phys. Soc. Jpn.* **73**, 2593 (2004) and contribution to this conference.
- (3) T.N. Ginter, K.E. Gregorich, W. Loveland, D.M. Lee, U.W. Kirbach, R. Sudowe, C.M. Folden III, J.B. Patin, N. Seward, P.A. Wilk, P.M. Zielinski, K. Aleklett, R. Eichler, H. Nitsche, and D.C. Hoffman, *Phys. Rev.* **C67**, 064609 (2003).
- (4) Yu.Ts. Oganessian, V.K. Utyonkov, Yu.V. Lobanov, F.Sh. Abdullin, A.N. Polyakov, I.V. Shirokovsky, Yu.S. Tsyganov, G.G. Gulbekian, S.L. Bogomolov, B.N. Gikal, A.N. Mezentsev, S. Iliev, V.G. Subbotin, A.M. Sukhov, A.A. Voinov, G.V. Buklanov, K. Subotic, V. I. Zagrebaev, M.G. Itkis, J.B. Patin, K.J. Moody, J.F. Wild, M.A. Stoyer, N.J. Stoyer, D.A. Shaughnessy, J.M. Kenneally, P.A. Wilk, R.W. Loughheed, R.I.II'kaev, and S.P. Vesnovskii, *Phys. Rev.* **C70**, 064609 (2004).
- (5) R. Smolanczuk, J. Skalski, and A. Sobiczewski, *Phys. Rev.* **C52**, 1871 (1995).
- (6) P. Möller, J.R. Nix, and K.L. Kratz, *Atomic Data and Nucl. Data Tables* **66**, 131 (1997).
- (7) R. Bass, *Nucl. Phys.* **A231**, 45 (1974).
- (8) W.D. Myers and W.J. Swiatecki, *Nucl. Phys.* **A601**, 141 (1996).
- (9) A. Sandulescu, R.K. Gupta, W. Scheid, and W. Greiner, *Phys. Lett.* **60B**, 225 (1976).
- (10) G.G. Adamian, N.V. Antonenko, and W. Scheid, *Phys. Rev.* **C69**, 14607 and 44601 (2004).
- (11) A.S. Zubov, G.G. Adamian, N.V. Antonenko, S.P. Ivanova, and W. Scheid, *Eur. Phys. J.* **A23**, 249 (2005).
- (12) Yu.Ts. Oganessian, A.V. Yeremin, G.G. Gulbekian, S.L. Bogomolov, V.I. Chepigin, B.N. Gikal, V.A. Gorshkov, M.G. Itkis, A.P. Kabachenko, V.B. Kutner, A.Yu. Lavrentev, O.N. Malyshev, A.G. Popeko, J. Rohac, R.N. Sagaidak, S. Hofmann, G. Münzenberg, M. Veselsky, S. Saro, N. Iwasa, and K. Morita, *Eur. Phys. J.* **A5**, 63 (1999).
- (13) Yu.Ts. Oganessian, A.V. Yeremin, A.G. Popeko, O.N. Malyshev, A.V. Belozero, G.V. Buklanov, M.L. Chelnokov, V.I. Chepigin, V.A. Gorshkov, S. Hofmann, M.G. Itkis, A.P. Kabachenko, B. Kindler, G. Münzenberg, R.N. Sagaidak, S. Saro, H.-J. Schött, B. Streicher, A.V. Shutov, A.I. Svirikhin, G.K. Vostokin, *Eur. Phys. J.* **A19**, 3 (2004).
- (14) A.B. Yakushev, I. Zvara, Yu.Ts. Oganessian, A.V. Belozero, S.N. Dmitriev, B. Eichler, S. Hübener, E.A. Sokol, A. Türler, A.V. Yeremin, G.V. Buklanov, M.L. Chelnokov, V.I. Chepigin, V.A. Gorshkov, A.V. Gulyaev, V.Ya. Lebedev, O.N. Malyshev, A.G. Popeko, S. Soverna, Z. Szegłowski, S.N. Timokhin, S.P. Tretyakova, V.M. Vasko, and M.G. Itkis, *Radiochim. Acta* **91**, 433 (2003).
- (15) K.E. Gregorich, W. Loveland, D. Peterson, P.M. Zielinski, S.L. Nelson, Y.H. Chung, Ch.E. Düllmann, C.M. Folden III, K. Aleklett, R. Eichler, D.C. Hoffman, J.P. Omtvedt, G.K. Pang, J.M. Schwantes, S. Soverna, P. Sprunger, R. Sudowe, R.E. Wilson, and H. Nitsche, *Phys. Rev.* **C72**, 014605 (2005).
- (16) B. Lommel, D. Gembalies-Datz, W. Hartmann, S. Hofmann, B. Kindler, J. Klemm, J. Kojouharova, and J. Steiner, *Nucl. Instrum. Methods* **A480**, 16 (2002).
- (17) R. Mann, D. Ackermann, S. Antalic, H.G. Burkhard, P. Cagarda, D. Gembalies-Datz, W. Hartmann, F.P. Heßberger, S. Hofmann, B. Kindler, P. Kuusiniemi, B. Lommel, S. Saro, H.G. Schöt, and J. Steiner, *GSI Scientific Report 2004-1*, 224 (2004).
- (18) E.K. Hulet, *Physics of Atomic Nuclei* **57**, 1099 (1994).
- (19) D.C. Hoffman and M.R. Lane, *Radiochim. Acta* **70/71**, 135 (1995).